

ORAL SESSION: BIOSENSORS 2

CROSS SELECTIVITY IMMUNOAFFINITY AND NEW APPLICATIONS FOR LACTOFERRIN IMMUNOSENSOR

M. Tomassetti, E. Martini, L. Campanella

Department Chemistry of University "La Sapienza", P.le a. Moro 5, 00185, Rome.

mauro.tomassetti@uniroma1.it

Abstract

We recently developed several different kinds of lactoferrin immunosensor. Initially we developed competition immunosensors using different transducers and two measurement geometries [1, 2]. More recently we developed a new direct method of measurement which allows a considerable reduction in analysis time [3].

The study was then extended to the ability of the antibody used and the analyte under test to produce the immunocomplex. As the immunoaffinity characteristic of the antigen for the immunoreagent is of the utmost importance in any immunological method, a rough estimation of the K_{aff} of the antigen under test (i.e. lactoferrin) was obtained by us at the midpoint of the Langmuir curve, where $K_{\text{aff}} = 1/IC_{50}$. In our case IC_{50} was calculated as the concentration of analyte that binds 50% of the antibody to the sensor surface. The K_{aff} value was found to be of the order of 10^6 M^{-1} in all cases, i.e. using different measurement geometries, different transducers and different methods, in either "direct" or "competition" mode (see figure 1).

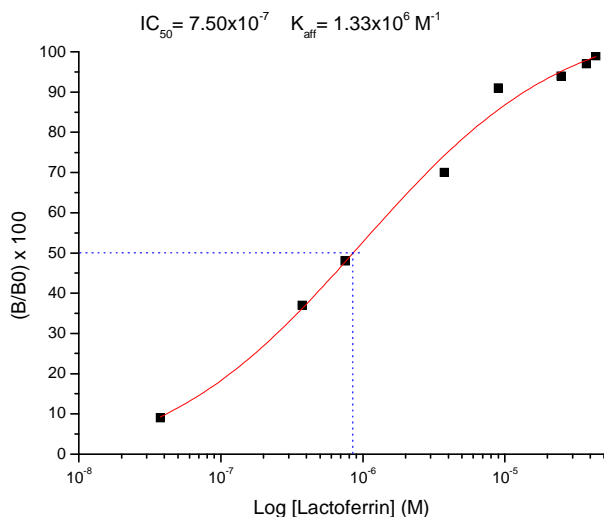


Figure 1. Example of IC_{50} and K_{aff} determination by Langmuir curve using the "direct" method and H_2O_2 electrode as transducer

In addition we studied the selectivity features with reference to other possible interfering milk or saliva proteins.

This study was performed in two ways. First we compared immunosensor response versus the same fixed concentration of lactoferrin and other proteins i.e. casein, human and bovine lactoglobulin, lactalbumin, IgG and IgA. We then experimentally determined and compared the cross selectivity values for all these proteins.

Lastly, we carried out new measurements using immunosensors on several real matrices such as powdered milk samples, saliva and tears, obtaining satisfactory results in all cases.

It was found that in samples of common powdered milk used as infants' food, lactoferrin content is about 10 times lower than in analogous samples, in which the manufacturer added lactoferrin to the product in order to bring the content of this protein in the sample closer to the values of lactoferrin contained in fresh human milk.

This provides a significant indicator of the importance that pharmaceutical firms operating in the infant food sector are currently attributing to this polyfunctional protein.

In conclusion, it is interesting to note that lactoferrin concentration in saliva does not differ appreciably from that of powdered milk [1], while its concentration in tears is higher by nearly three orders of magnitude.

REFERENCES

1. L. Campanella, E. Martini, M. Tomassetti. *J. Pharm. Biomed. Anal.* 48 (2008), 278–287.
2. L. Campanella, E. Martini, M. Pintore, M. Tomassetti. *Sensors* 9 (2009), 2202-2221.
3. L. Campanella, E. Martini, M. Tomassetti, Abstract book page 77, 13th International Meeting RDPA 2009, 9-12 September, Milan, Italy.

ONE-DIMENSIONAL POLYANILINE NANOTUBES FOR ENHANCED MOLECULARLY IMPRINTED POLYMER-BASED SENSING

Francesca Berti*, Giovanna Marrazza, Marco Mascini

Department of Chemistry, University of Florence, Via della Lastruccia 3, 50019 Sesto Fiorentino, Italy.

Silvia Todros, Matteo Ferroni, Guido Faglia

CNR - INFM SENSOR Laboratory, Department of Chemistry and Physics, University of Brescia, via Valotti 9, 25133 Brescia, Italy.

Dhana Lakshmi, Iva Chianella, Michael J. Whitcombe, Sergey Piletsky, Anthony P. F. Turner
Cranfield Health, Cranfield University, Cranfield, Bedfordshire, MK43 0AL, UK.

Abstract

Over the past decade, significant progress has been made in utilising cutting-edge techniques associated with nanomaterials and nano-fabrication to expand the scope and capability of biosensors to a new level of novelty and functionality.

In this work we explored a simple, cheap and fast route to grow polyaniline (PANI) nanotubes arranged in an ordered structure directly on an electrode surface by electrochemical polymerisation, using an alumina nanoporous membrane as a template (Figure 1). Among conducting polymers, polyaniline has generated great interest because it is inexpensive, easy to process and dope, has high conductivity and the raw materials for its synthesis are readily available.

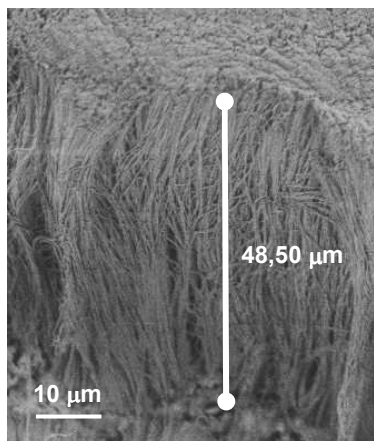


Figure 1. Vertically aligned PANI nanostructures, cross-sectional view.

The deposited nanostructures were electrochemically and morphologically characterised and then used as a functional substrate for the development of a molecularly imprinted polymer-based sensor. Thus, we were able to exploit the intrinsic advantages of nanostructures as optimal transducers and the well known benefits of molecularly imprinted polymers (MIPs) as receptors. A novel hybrid material, N-phenylethylene diamine methacrylamide (NPEDMA) was employed as monomer, combining two orthogonal polymerisable functionalities, an aniline group and a methacrylamide¹. In this way, the polymerisation of NPEDMA resulted in a conductive layer which allowed direct electrical connection between the electrode and the MIP.

The hybrid nanostructured-MIP sensor was applied to the molecular recognition of catechol (Figure 2). Compared to an analogue non-nanostructured sensor, the detection limit was one order of magnitude lower.

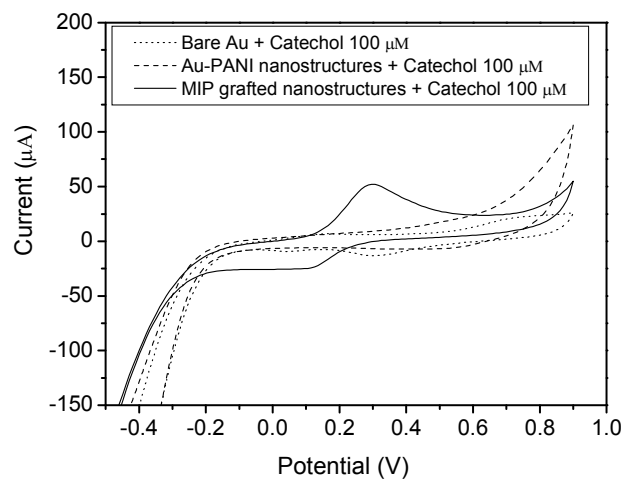


Figure 2. Voltammetric scans of Catechol 100 μ M in PBS. Signals obtained using MIP-grafted sensor (solid line), Au-sputtered alumina membrane before electro-polymerisation (dotted line), sensor after growth of PANI nanostructures (dashed line). Oxidation and reduction peaks are visible only when using a MIP-grafted sensor.

REFERENCES

1. D. Lakshmi, M. J. Whitcombe, F. Davis, I. Chianella, E. V. Piletska, A. Guerreiro, S. Subrahmanyam, P. S. Brito, S. A. Fowler, S. A. Piletsky, *Chem. Commun.*, 19 (2009), 2759.

CORRESPONDING AUTHOR: e-mail: francesca.beriti@unifi.it, Phone: +39 055 4573373.

MODIFIED CARBON NANOTUBES FOR INTRACELLULAR pH SENSING

A. Giannetti, **G. Ghini**, C. Trono, F. Baldini

*Istituto di Fisica applicata "Nello Carrara" (IFAC-CNR), via Madonna del Piano 10,
50019 Sesto Fiorentino (FI), Italy*

G. Puleo, G. Giambastiani

*Istituto di Chimica dei Composti OrganoMetallici (ICCOM-CNR), via Madonna del Piano 10,
50019 Sesto Fiorentino (FI), Italy*

Abstract

The use of carriers for the intracellular drug delivery or for the transportation of drugs in target tissues, difficult to get in normal conditions, is a well-known strategy and often indispensable for the achievement of effective therapeutic results. A more recent but equally promising application is given by the delivery of optical nanosensors capable to monitor in real time chemical and biochemical parameters inside the cells. With the sensor embedded inside the cell, it is possible to control its vital functions, as well as the effect of administered drugs. These nanosensors use fluorescent transducers chemically bound to nanostructures able to enter the cells, which change their fluorescence with the change of the concentration of the parameter of interest.

Carbon nanotubes are among the novel emerging technologies with potential application for the molecule delivery inside the cells and they can be a valid alternative to the nanostructures utilised up to now, such as quantum dots and gold or silica nanoparticles. The small dimensions of carbon nanotubes, combined with their remarkable physical, mechanical and electrical properties, make them a unique material [1]. These biomedical applications can be envisaged thanks to the functionalization of the surface that brings to a high soluble material [2].

In this work multi-walled carbon nanotubes (MWCNTs) are proposed as macromolecular carriers for pH detection inside the cells. Different ethylen-glycol fluorescein derivates were covalently bound to carboxyl functionalized MWCNTs. Ether chains were bound in the correspondence of the carboxylic group of the dye, paying attention not to affect its fluorescence properties and its pH dependence. The ether spacers have a twofold function: i) to separate the dye from the nanotube in order to prevent the fluorescence quenching; ii) to provide a better water solubility of the final product.

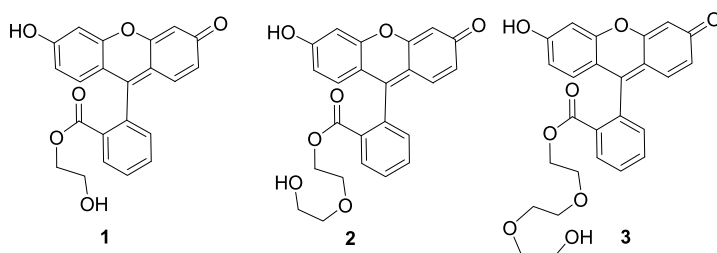


Figure 1. Fluorescein-carboxyl derivates with spacers of different length

The presence of the dye bound on MWCNTs was demonstrated by infrared spectra that show the characteristic absorption bands of the carboxyl ester groups and of the ether chain of the dye. Elementary analysis performed on the achieved samples revealed a ratio of 0.018mmol of dye per 100mg of sample. The pH dependence of the modified nanotubes was analysed in an aqueous solution of MWCNT-derivates, after suitable sonication. The pH of the solution was adjusted in the range 4-9 pH units by adding drops of hydrochloric acid and sodium hydroxide. Dye excitation was

obtained by means of a LED with peak emission at 490 nm filtered by a band-pass filter (10 nm FWHM) at 488 nm. An optical fiber (core diameter = 1 mm) positioned at 90° with respect of the excitation beam direction, was connected with a Hamamatsu spectrum analyzer for the recording of the fluorescence spectra. MWCNTs derivated with fluorescein 2 showed the best results. The modified MWCNTs exhibited linear pH dependence in the range between 5.5 pH and 7.5 pH units with a sensitivity less than 0.1 pH units (Figure 2).

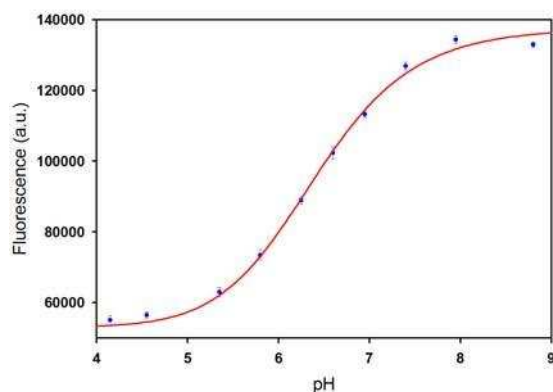


Figure 2. Experimental pH dependence for MWCNTs carrying fluorescein 2.

Recent promising results were also achieved immobilising the dye calcein, a cation-sensitive fluorophore (H^+ , Ca^{2+} , Fe^{2+} ...), by covalent bond with amino-functionalised MWCNTs (Figure 3). Preliminary characterisation of these modified MWCNTs in the presence of pH changes shows higher fluorescence levels, as shown in Figure 4.

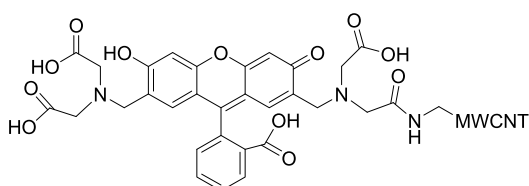


Figure 3. Schematic representation of calcein dye linked to the amino-functionalised MWCNT

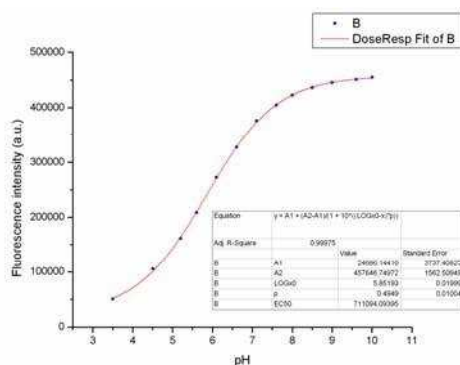


Figure 4. Experimental pH dependence for MWCNTs carrying calcein

This research study was supported by the Regional Project ICT-ONE. MWCNTs were provided by NANOCYL.

REFERENCES

1. M.Kohler, W.Fritzsche, Nanotechnology, An Introduction to nanostructuring techniques. Weinheim, Germany, Wiley-VCH, 272, 2004.
2. K.Kostarelos, L.Lacerda, G.Pastorin, Wei Wu, S.Wieckowski, A.Luangsilavay, S.Godefroy, D.Pantarotto, J-P.LBriand, S.Muller, M.Prato, A.Bianco, Nature Nanotechnology, 2 (2007) 108

NEW HYBRID RESONATOR FOR BIOSENSING APPLICATIONS

C. Ciminelli, C. Campanella, M. N. Armenise

Laboratorio di Optoelettronica, Politecnico di Bari, Via E. Orabona n.4, 70125, Bari, Italy

Abstract

Microresonant cavity-based integrated optical devices have been widely investigated in order to realize a variety of devices such as lasers, sensors, optical switches and add-drop filters.

In the last decade, different platforms for optical sensing, as interferometers, optical waveguides, surface plasmon resonance devices and optical ring resonator-based biosensors, have been proposed. In particular, the peculiarity of microresonant biosensors is that they have small dimensions, high sensitivity, high capability of integration onto a chip and are potentially well suitable for mass-production.

Light coupled to microcavities is confined within the structure by the physical phenomenon of the “total internal reflection” (TIR), forming high quality factor (Q) resonant modes.

Any interaction with the evanescent tail of the optical field affects the guided-mode, so inducing a shift in the resonant wavelength. This resonance change can be detected with very high sensitivity by optimizing the microcavity design and the method of observation.

Optical characteristics of two standard SOI (Silicon on Insulator) microresonators, a ring- and a disk-resonator (see Fig.1), coupled to two separate bus waveguides have been investigated both theoretically and experimentally.

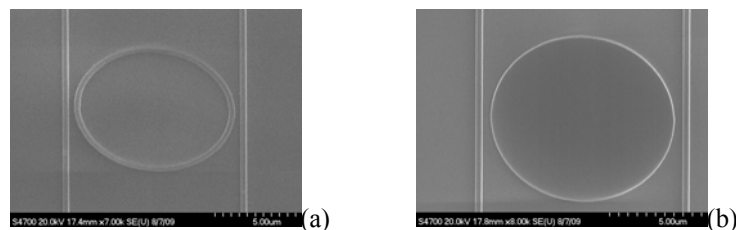


Figure 1 – Microring (a) and microdisk (b) resonator coupled to two bus waveguides.

The physical dimensions (width = 500nm, thickness = 220nm) of the waveguides have been determined in order to excite a TE_0 mode when a source light with a wavelength in the range $1.52\div 1.59\mu\text{m}$ is applied; effective index calculated for the TE_0 mode is 2.6. The radius of both microdisk and microring resonator has been fixed to $5\mu\text{m}$, while the gap between the microcavity and the waveguides has been varied from 100 nm to 500 nm in order to achieve the biggest possible value of the Q-factor. The optical properties of both microresonators have been investigated via a 2D Finite Differences Time Domain (FDTD) method by setting the frequency resolution to 30pm. It results that as the gap increases, the Q-factor increases too and the coupled power decreases. A Q-factor of $3\cdot 10^4$ has been calculated for the microring, while $5\cdot 10^4$ is the microdisk Q-factor with a gap of 300nm for both resonators.

The inner area of the ring resonator has been supposed to be filled with different analytes. A shift, $\Delta\lambda_{\text{res}}$, in the fundamental mode resonance has been observed and the sensitivity has been calculated as the ratio $\Delta\lambda_{\text{res}}/\Delta n$, with Δn the change in the refractive index of the analyte.

The obtained results induced us to investigate about the optical behaviour of a new shape, named

“hybrid resonator”. This microresonator has a geometry similar to that of a ring resonator and a Q-factor similar to the one of a microdisk (bigger than the microring one, for fixed radius R, gap and waveguides width, Fig. 2.a).

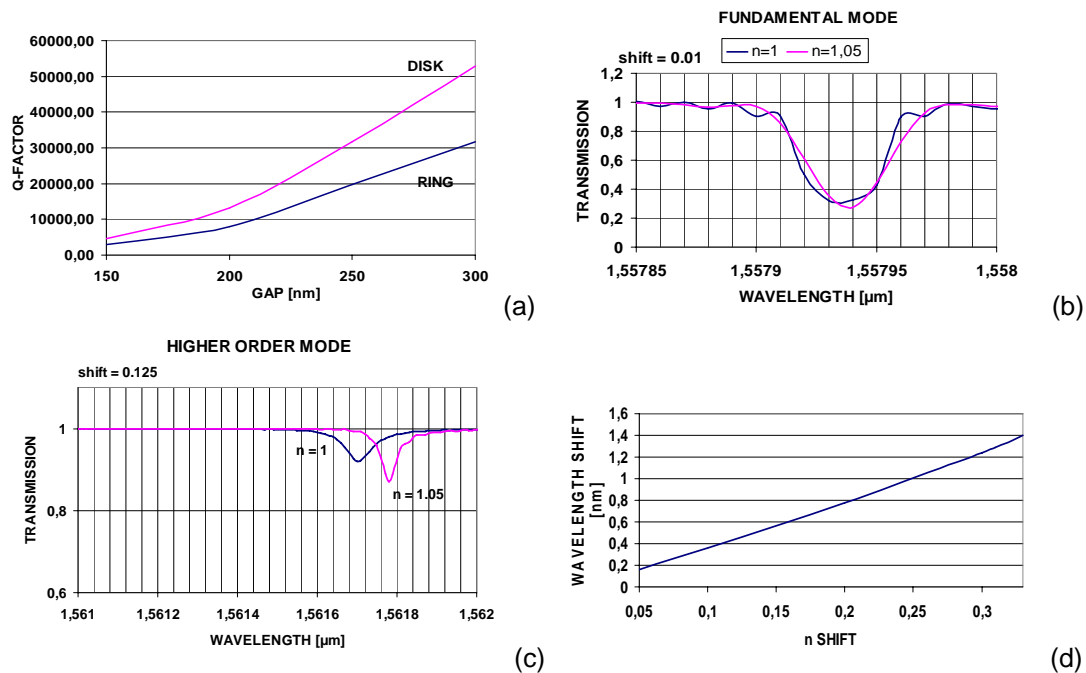


Figure 2 – (a) Comparison between the quality factor Q of microring and microdisk resonators. (b) and (c) Fundamental mode and higher order mode resonance shift, $\Delta R = 1\mu\text{m}$, respectively. (c) Relationship between the resonance shift and the effective index shift.

To study the new resonator configuration, the ring width (defined as the difference ΔR between the outer radius and the inner radius) has been varied until the “hybrid structure” optical properties became similar to the ones of the disk-resonator. For a waveguide width of 500nm, several configurations have been investigated; the limit-value beyond the hybrid resonator Q-factor is comparable to the disk Q-factor has been found to be $\Delta R = 2\mu\text{m}$. If $\Delta R \geq 2\mu\text{m}$, the wavelength shift does not affect the fundamental mode, but higher order modes, so it is not useful for sensing.

The width for which the ring shows good values of sensitivity and Q-factor ($Q = 4 \cdot 10^4$) is $\Delta R = 750\text{nm}$ when the resonator outer radius is $5\mu\text{m}$, the waveguides width is 500nm and the gap is 300nm. If different kinds of analyte are investigated, the existing relation between the resonance shift and the refractive index is linear (Fig. 2.c).

The microresonators have then been fabricated and preliminary results confirmed the new resonator configuration well suitable for sensing applications, as above demonstrated.

REFERENCES

1. Ayc,a Yalc,m, Ketul C. Papat, John C. Aldridge, Tejal A. Desai, John Hryniewicz, Nabil Chbouki, Brent E. Little, Oliver King, Vien Van, Sai Chu, David Gill, Matthew Anthes-Washburn, B. Goldberg, ‘Optical sensing of biomolecules using microring resonators’, IEEE, Vol.12, NO. 1, January/February 2006.
2. Xudong Fan, Ian M. White, Siyka I. Shopova, Hongying Zhu, Jonathan D. Suter, Yuze Sun, “Sensitive optical biosensors for unlabeled targets: A review”, ELSEVIER, Analytica Chimica Acta 6 2 0, pp.8–26, 2008.
3. H.S.Lee, B.H.O, S.G.Lee, E.H.Lee, “Design of a silicon optical micro-ring resonator sensor of improved sensitivity and selectivity”, Optoelectronic Integrated Circuits X, Proceedings of the SPIE, vol. 6897, pp. 68970W-13, 2008.
4. C. Campanella, “Design and fabrication of an optical cavity resonator based sensor”, Master thesis in Automation Engineering, Politecnico di Bari, 2009.

A PIEZOELECTRIC QUARTZ CRYSTAL SENSOR APPLIED FOR TROMBIN-BINDING APTAMERS

Jano Rakitka, **Tibor Hianik** *

**Department of Nuclear Physics and Biophysics, Comenius University, Mlynska dolina F1, 84248
Bratislava, Slovakia e-mail: tibor.hianik@fmph.uniba.sk.*

Ilaria Lamberti, Lucia Mosiello

*ENEA, Italian National Agency for New Technologies, Energy and the Environment Via Anguillarese 301,
00060 Rome, Italy e-mail: Lucia.mosiello@enea.it; Ilaria.lamberti@enea.it*

Abstract

Biosensors based on DNA or RNA aptamers (aptasensors) represent new type of the sensor that utilize unique properties of artificial receptor – aptamers. Aptasensors are of considerable interest due to their application in detection practically unlimited kind of compounds [1]. Aptamers are single-stranded RNA or DNA oligonucleotides 15 to 60 base in length that bind with high affinity to specific molecular targets such as nucleic acid, proteins, small compounds or cells. Their specificity is comparable and in certain cases even higher than those of antibodies. In contrast to antibodies, aptamers are prepared by in vitro selection procedure (SELEX) developed simultaneously in early 1990s by L. Gold and A. Ellington laboratories [2]. Among aptamers those specific to the thrombin were most extensively studied. Thrombin is a multifunctional serine protease, which plays an important role in pro-coagulant and anti-coagulant function. This protease converts soluble fibrinogen into insoluble strands of fibrin, which is responsible either for a physiological plug or pathological thrombus. Thrombin has two binding site that are spatially separated and localized at opposite poles of thrombin molecules. These binding sites are sensitive to fibrinogen and heparin, respectively. Aptamers can be used as potential inhibitors of thrombin, therefore study of the mechanisms of interaction of thrombin with aptamers is of great importance for medicine.

The aim of our work was to analyze the binding of human thrombin to the DNA aptamers that differ in structure of binding site. As a basic we used aptamer that selectively bind thrombin in its fibrinogen-binding site. The composition of the aptamer was as follows: Conventional aptamer sensitive to fibrinogen binding site: d(T₁₅GG**TT**GGTGTGGTTGG). (TT aptamer) (Bock et al. [3] have developed this aptamer). The underlined bold pair of thymines is responsible for binding the thrombin. We analysed also aptamers in which AA replaced TT pair, AT or TA (AA, AT or TA aptamers, respectively). The aptamers were purchased from Thermo Scientific (Ulm, Germany). We used acoustic method based on quartz crystal microbalance (QCM) and thickness shear mode (TSM) for monitoring the aptamer-thrombin interaction. The QCM method is based on measurement of resonant frequency of the quartz transducer. The application of an external electrical potential to a piezoelectric material produces internal mechanical stress. In a piezoelectric sensor, an oscillating electric field applied across the device induces an acoustic wave that propagates through the crystal and meets minimum impedance when the thickness of the device is a multiple of a half wavelength of the acoustic wave. Deposition of a thin film on the crystal surface decreases the frequency in a portion to the mass of the film [4]. However exact relation between the changes of the resonant frequency and mass is according to Sauerbrey [5] valid only for dry crystal. In a solution, the contribution of viscoelasticity should be considered due to the possible friction between the bilayer at crystal surface and surrounding liquid. The analysis of viscoelastic contribution can be made by TSM method. This method is based on analysis of complex impedance spectra of quartz transducer. In addition to the resonant frequency also so called motional

resistance, R_m , can be determined in this method. The R_m value is measure of viscoelastic contribution to the crystal oscillation [6]. The sensor has been prepared by immobilisation of biotinylated DNA aptamers onto the gold surface of the quartz with chemisorbed neutravidin. Due to high affinity of biotin to neutravidin a stable aptamer layer was formed at the crystal surface. As a binding buffer we used 20 mM Tris; 140 mM NaCl; 5 mM KCl; 1 mM $MgCa_2$; 1 mM $MgCl_2$, pH 7.4. The experiments were performed as follows. The clean crystal has been placed into the flow cell. The neutravidin (0,2 mg/mL) has been allowed to flow to the surface. The decrease of resonant frequency and slight increase of motional resistance were observed. After the parameters were stabilised the biotinylated aptamers in a concentration of 2 μ M were added. This resulted further frequency decrease and in more remarkable increase of motional resistance in comparison with those for neutravidin layer. This suggests substantial viscosity contribution. After stabilization of acoustic parameters the thrombin has been added in a concentration range 30 to 300 nM. This resulted also in frequency decrease and in changes of motional resistance that depended on the aptamers structure. Most remarkable differences in the acoustic parameters following addition of thrombin were observed for conventional (TT) and AA aptamers. The resonant frequency for both aptamers decreased with increasing thrombin concentration. However, for TT aptamers these changes were substantially larger, which suggest stronger interaction of thrombin. Substantial differences were observed in motional resistance changes, that were opposite for both aptamers. While for TT aptamers the motional resistance increased with increasing the thrombin concentration, opposite changes in R_m took place for AA aptamers. This suggests different conformation/surface properties of the thrombin-aptamer complexes for TT and AA aptamers.

REFERENCES

1. Hianik, T., and Wang, J. (2009) *Electroanalysis*, 21:1223-1235
2. Ellington, A.D., and Szostak, J.W (1990), *Nature* 346: 818-822.
3. Bock, L.C., Griffin, L.C., Latham, J.A. Vermaas, E.H. and Toole J.J. (1992), *Nature* 355: 564-566.
4. O'Sullivan CK and Guilbault GG (1990) *Biosensor & Bioelectronics* 14: 663-670
5. Sauerbrey, G. (1959), *Z. Phys.* 155: 206–210.
6. Hianik, T., Grman, I. and Karpisova, I. (2009) *Chem. Commun.* 6303–6305.